

# Molecular Dynamics Simulation of an Aqueous $\text{MgCl}_2$ Solution. Structural Results

W. Dietz, W. O. Riede, and K. Heinzinger

Max-Planck-Institut für Chemie (Otto-Hahn-Institut), Mainz, Germany

Z. Naturforsch. **37a**, 1038–1048 (1982); received June 12, 1982

A molecular dynamics simulation of a 1.1 molal aqueous  $\text{MgCl}_2$  solution has been performed employing the central force model for water. The effective pair potentials for ion-water have been derived from ab initio calculations. The basic box with a sidelength of 18.30 Å contained 200 water molecules, 8 anions and 4 cations, corresponding to an experimental density of 1.079 g/cm<sup>3</sup>. The simulation extended over about 3.3 picoseconds at an average temperature of 309 K. The structure of the solution is described by radial distribution functions and the orientation of the water molecules in respect to physically meaningful directions. Values for the dielectric constant and hydration energies have been calculated. The strong influences of the twofold charged magnesium ion on the geometry of the water molecules and the structure of the hydration shell is discussed in comparison with the results of a previous simulation of a 2.2 molal NaCl solution.

## I. Introduction

In recent years a number of computer simulations has been performed on aqueous solutions of 1-1 electrolytes. As a consequence a lot of detailed information on the structure and dynamics of these solutions has become available. Therefore it was of great interest to extend molecular dynamics (MD) computer simulations to solutions containing two-fold charged ions.

The  $\text{MgCl}_2$  solution was chosen because the size of the cation is very similar to that of  $\text{Li}^+$ , which has been studied recently in an MD-simulation of a 2.2 molal  $\text{LiI}$  solution [1]. It was interesting to investigate how the doubled charge influences the properties of the hydration shells of  $\text{Mg}^{++}$ . Investigations on the structure of  $\text{MgCl}_2$  solutions by x-ray measurements, which have been reported in literature [2, 3], provide a good basis for comparison with the MD-results. Furthermore, the existence of three stable isotopes of Mg makes the  $\text{MgCl}_2$  solution very suitable also for neutron diffraction experiments, which provide even more detailed information on the structure of the solution by the method of isotopic substitution [4] than x-ray does.

The central force (CF) model for water [5] is used, which has been applied before successfully in the MD-simulation of a 2.2 molal NaCl solution [6]. In this model the three atoms of the water molecule interact also internally by appropriate hydrogen-

hydrogen and hydrogen-oxygen pair potentials, which enable the occurrence of the three vibration modes of the molecule. The dependance of these vibrations on the different surroundings in the solution will be reported in a second paper on dynamical properties of the  $\text{MgCl}_2$  solution. Also the average water geometry will be influenced by the interactions with the ions and the other water molecules, thus reproducing to a certain extend the polarization effects.

In this paper the structure of the  $\text{MgCl}_2$  solution is discussed on the basis of the different radial distribution functions. The orientations of the water molecules are compared with the results from an MD-simulation of 2.2 molal NaCl solution [6]. Within this context the dielectric constants according to the Onsager-Kirkwood model [7] have been evaluated. From potential energy relationships the hydration energies for the different ions have been calculated.

## II. Details of the Simulation

In the MD simulation of an aqueous 1.1 molal  $\text{MgCl}_2$  solution the basic cube contains 200 water molecules, 4 cations and 8 anions. The experimental density of 1.079 g/cm<sup>3</sup> corresponds to a side length of 18.30 Å.

The central force model of water [5] is employed, which describes the intra- and intermolecular O–H and H–H interactions by the same pair potential. Thus the interactions of the four kinds of particles

Reprint requests to Dr. K. Heinzinger, Max-Planck-Institut für Chemie, Saarstraße 23, D-6500 Mainz.

0340-4811 / 82 / 0900-1038 \$ 01.30/0. — Please order a reprint rather than making your own copy.



Dieses Werk wurde im Jahr 2013 vom Verlag Zeitschrift für Naturforschung in Zusammenarbeit mit der Max-Planck-Gesellschaft zur Förderung der Wissenschaften e.V. digitalisiert und unter folgender Lizenz veröffentlicht: Creative Commons Namensnennung-Keine Bearbeitung 3.0 Deutschland Lizenz.

Zum 01.01.2015 ist eine Anpassung der Lizenzbedingungen (Entfall der Creative Commons Lizenzbedingung „Keine Bearbeitung“) beabsichtigt, um eine Nachnutzung auch im Rahmen zukünftiger wissenschaftlicher Nutzungsformen zu ermöglichen.

This work has been digitalized and published in 2013 by Verlag Zeitschrift für Naturforschung in cooperation with the Max Planck Society for the Advancement of Science under a Creative Commons Attribution-NoDerivs 3.0 Germany License.

On 01.01.2015 it is planned to change the License Conditions (the removal of the Creative Commons License condition “no derivative works”). This is to allow reuse in the area of future scientific usage.

– O, H,  $\text{Mg}^{++}$ , and  $\text{Cl}^-$  – are determined by ten pair potentials which depend only on their mutual distances. Each of the ten pair potentials  $V_{\alpha\beta}(r)$  consists of a coulombic term and a second term describing the interactions which do not depend explicitly on the charges:

$$V_{\alpha\beta}(r) = q_\alpha q_\beta / r + V'_{\alpha\beta}(r). \quad (1)$$

The charges  $q_\nu$  are  $0.3298|e|$ ,  $-0.6597|e|$ ,  $-1.0|e|$ , and  $2.0|e|$  for the hydrogen, oxygen, chlorine, and magnesium, respectively.

In the simulation both parts of the potential and the corresponding forces are treated in different ways. For the coulombic part the method of Ewald summation is employed. The other part of the potential is taken in account only if the distance of the two interacting particles is smaller than the cut off radius  $r_c$ . If a particle is crossing the cut off sphere this simple procedure leads to jumps in energy and force thus generating trends in the average kinetic energy. This deficiency can be avoided if  $V'_{\alpha\beta}(r)$  is modified according to the "shifted force potential" method [8].

In the version used here the force is shifted to zero at the cut off distance  $r_c$  by adding a suitable constant force. At distances greater  $r_c$  the modified force is zero by definition. The corresponding modified potential is obtained by integration of the force. The constant of integration can be chosen in such a way that the potential equals also zero at the cut off radius. The three potentials  $V_{\text{OO}}$ ,  $V_{\text{OH}}$ , and  $V_{\text{HH}}$  of the "Central Force" water model are the same as used by Rahman and Stillinger [5] in an MD simulation of pure water, and in a previous simulation of a 2.2 molal NaCl solution [6]. The four ion-water potentials  $V_{\text{MgO}}$ ,  $V_{\text{MgH}}$ ,  $V_{\text{ClO}}$ ,  $V_{\text{ClH}}$  consist of a coulombic term, and  $1/r^2$ -term, and an exponential term. The derivation of these potentials was based on ab initio energy calculations of different ion-water configurations.

In the case of  $\text{Cl}^-$ - $\text{H}_2\text{O}$  sufficient ab initio data are available from the literature [9]. For  $\text{Mg}^{++}$ - $\text{H}_2\text{O}$  only a small number of ab initio data is reported [10–12]. The purpose of these investigations was mainly the evaluation of the dissociation energy. As a consequence only configurations with  $C_{2v}$ -symmetry have been studied, which is not sufficient to derive a reliable potential for all possible ion-water arrangements that will occur in the solution. Therefore we performed ab initio calculations

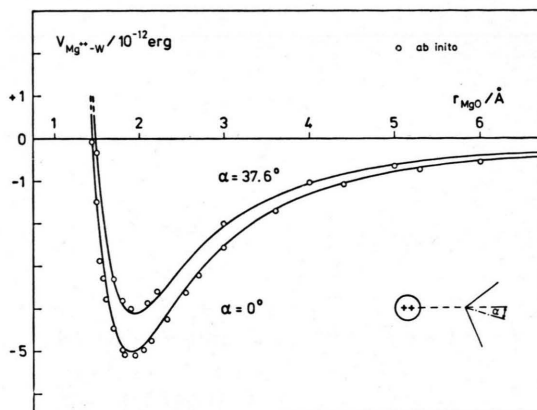


Fig. 1.  $\text{Mg}^{++}$ -water pair potentials calculated with  $V_{\text{MgO}}(r)$  and  $V_{\text{MgH}}(r)$  (see Table 1) as a function of the ion-oxygen distance for the orientations shown in the insertion. The geometry of the isolated water molecule is  $r_{\text{OH}} = 0.957 \text{ \AA}$  and  $\angle \text{HOH} = 104.5^\circ$ . Circles indicate energy values from ab initio calculations.

for different  $\text{Mg}^{++}$ - $\text{H}_2\text{O}$  configurations. A greater number of energetically favourable arrangements and a smaller number of less probable ones was chosen to provide a reasonable basis for the potential fit. A detailed description is given in Appendix A. In Fig. 1 the  $\text{Mg}^{++}$ - $\text{H}_2\text{O}$  pair potentials are drawn for two planar configurations.

The fit procedure for the ion oxygen and ion-hydrogen pair potentials was similar to the one described in the previous paper on the simulation of the aqueous NaCl solution: After subtracting the coulombic contributions for the various ion-water configurations from the ab initio energies the analytical shifted force potentials were fitted to the remaining values.

The ion-ion pair potential is also derived on the basis of ab initio energy values. Its analytical form is the same as the ion-oxygen and ion-hydrogen pair potential except for the  $1/r^2$ -term, which is replaced in the case of  $\text{Cl}^-$ - $\text{Cl}^-$  and  $\text{Mg}^{++}$ - $\text{Mg}^{++}$  by an  $1/r^6$ -term. All pair potentials in the unmodified form are given in Table 1. The "shifted force potentials" can be derived easily from the unmodified ones.

The starting configuration for the simulation of the 1.1 molal  $\text{MgCl}_2$  solution was derived from a configuration of the simulation of a 2.2 molal NaCl solution. For this purpose four cations have been removed and the remaining four  $\text{Na}^+$  were replaced by  $\text{Mg}^{++}$ . After this manipulation the system was equilibrated during a few thousand time steps before the collection of data was started.

Table 1. Pair potentials employed in the MD simulation of an 1.1 molal MgCl<sub>2</sub> solution with  $r$  in Å and  $V$  in units of  $10^{-12}$  erg. The cut off distances in units of the box side-length 18.3 Å are 0.45, 0.22, and 0.16 for  $V_{OO}$ ,  $V_{OH}$ , and  $V_{HH}$  and 0.5 for the other pair potentials.

$V_{OO}(r)$	$= 10.04/r + 1858/r^{8.86} - 1.736 \cdot 10^{-2} \cdot \{\exp[-4(r-3.4)^2] + \exp[-1.5(r-4.5)^2]\}$
$V_{OH}(r)$	$= -5.019/r + 0.433/r^{9.2} - 0.694/\{1 + \exp[40(r-1.05)]\} - 0.278/\{1 + \exp[5.493(r-2.2)]\}$
$V_{HH}(r)$	$= 2.509/r + 2.251/\{1 + \exp[40(r-2.05)]\} - 1.181 \exp[-7.622(r-1.4525)^2]$
$V_{MgO}(r)$	$= -30.44/r - 14.79/r^2 + 4475 \exp(-4.08 r)$
$V_{MgH}(r)$	$= 15.22/r + 1.362/r^2 + 1.226 \exp(-0.349 r)$
$V_{ClO}(r)$	$= 15.22/r - 1.849/r^2 + 6304 \exp(-3.21 r)$
$V_{ClH}(r)$	$= -7.609/r + 3.138 \cdot 10^{24} \exp(-34.0 r)$
$V_{MgMg}(r)$	$= 92.27/r - 24.57/r^6 + 3.026 \cdot 10^4 \exp(-6.36 r)$
$V_{MgCl}(r)$	$= -46.14/r - 33.32/r^2 + 1968 \exp(-2.65 r)$
$V_{ClCl}(r)$	$= 23.07/r - 476.1/r^6 + 1.523 \cdot 10^4 \exp(-3.39 r)$

Besides the modifications of the pair potentials described above the time step was shortened to  $0.25 \cdot 10^{-15}$  seconds compared to  $0.40 \cdot 10^{-15}$  seconds in the previous NaCl-simulation. These alterations caused an improvement of the stability of the energy of one order of magnitude. The whole simulation was extended over more than 13000 time steps equivalent to a total elapsed time of about 3.3 picoseconds. The velocities were not rescaled during the simulation in order to get reliable velocity autocorrelation functions. The mean temperature of the total system increased slightly from 306 K at the beginning to 309 K at the end of the simulation.

### III. Results and Discussion

#### A) Radial Distribution Functions (RDF)

In Fig. 2 the ion-oxygen and ion-hydrogen RDF's  $g_{\alpha\beta}(r)$  for the 1.1 molal MgCl<sub>2</sub> solution are drawn. Also the running integration numbers are shown, which are defined as

$$n_{\alpha\beta}(r) = 4 \pi \varrho \int_0^r g_{\alpha\beta}(r') r'^2 dr'$$

with  $\varrho$  the number density of the water molecules. Characteristic data of the  $g_{\alpha\beta}(r)$  are given in Table 2.

The magnesium-oxygen RDF shows a very sharp first peak centered at 2.0 Å. This value is about

0.1 Å shorter than the results from x-ray scattering [2]. The first hydration shell is very well defined and separated from the second one. The number of water molecules in it is exactly 6.0. No exchange of any water molecule between the first and second hydration shells was observed in the course of the simulation. This is as expected for such strong ion solvent interactions.

The region from about 3.5 Å up to about 5.0 Å shows the second hydration shell with its maximum value at a distance of about 4.6 Å. The number of water molecules belonging to it can be given approximately with  $15 \pm 1$  because of the less pronounced second minimum. Behind the second shell there remains still some structure in  $g_{MgO}(r)$  which might indicate even a weekly pronounced third one. Further insight into the structure of the second hydration shell will be provided by the investigation of the orientation of the water molecules in respect to the ions.

The cation-hydrogen RDF shows a less but nevertheless well pronounced peak at 2.75 Å containing all the twelve hydrogens of the six hydration

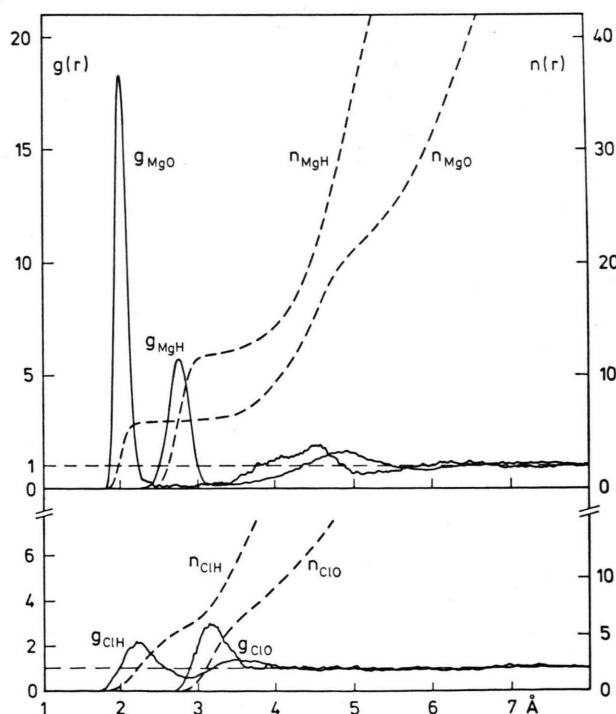


Fig. 2. Ion-oxygen and ion-hydrogen radial distribution functions (full) and running integration numbers (dashed) for a 1.1 molal MgCl<sub>2</sub> solution.



Table 2. Characteristic values for the radial distribution functions  $g_{\alpha\beta}(r)$  for the 1.1 molal  $\text{MgCl}_2$  solution.  $R_i$ ,  $r_{M_i}$  and  $r_{m_i}$  give the distances in Å, where for the  $i$ th time the  $g_{\alpha\beta}(r)$  is unity, has a maximum and a minimum, respectively. For O-H and H-H only intermolecular data are given.

$\alpha$	$\beta$	$R_1$	$r_{M1}$	$g_{\alpha\beta}(r_{M1})$	$R_2$	$r_{m1}$	$g_{\alpha\beta}(r_{m1})$	$r_{M2}$	$g_{\alpha\beta}(r_{M2})$	$n_{\alpha\beta}(r_{m1})$
Mg	O	1.86	2.00	19.2	2.23	2.3 ... 3.0	$\approx 0$	4.57	2.03	6.0
Mg	H	2.50	2.75	5.96	2.98	3.2 ... 3.3	0.09	4.90	1.67	12.0 (1)
Cl	O	2.89	3.18	2.88	3.63	—	—	—	—	7.0 (5)
Cl	H	1.97	2.25	2.25	2.60	2.86	0.57	3.50	1.37	6.0 (5)
O	O	2.59	2.82	3.00	3.13	3.4	0.75	4.63	1.15	4.95 (5)
O	H	1.81	1.92	1.23	2.03	2.48	0.23	3.15	1.48	4.0 (1)
H	H	2.14	2.20	1.74	2.69	3.03	0.78	3.65	1.18	6.5 (3)

shell water molecules. The subsequent region of the second hydration shell is also well resolved in  $g_{\text{MgH}}(r)$ .

The mean cation-oxygen distance (2.0 Å) is slightly greater than the distance of the minimum of the effective pair potential (see Fig. 10) for the corresponding water-cation orientation. This means that on the average the size of the cage formed by the six waters is determined by the size of the water molecules and is slightly greater than would be necessary for the central cation. Because of the sharp radial distribution of the cation-water distances a rather regular octahedron is expected for the hydration shell of  $\text{Mg}^{++}$ . In the case of the anion there is a significantly larger average Cl-water distance (3.18 Å) combined with a broader radial distribution. Because of the larger space available for the hydration water the anion hydration shell cannot be expected to exhibit such a geometrical structure as in the case of  $\text{Mg}^{++}$ .

But one has to keep in mind that liquids exhibit no rigid geometrical structures as might be suggested by values got from time and particle averages. Therefore it will be worth to investigate to which degree regular geometrical structures are actually realised. This will be done extensively in the subsequent paper [13].

The chlorine-oxygen RDF shows one single peak followed by a nearly uniform distribution. A similar shape of  $g_{\text{ClO}}(r)$  was found in a previous simulation of a 2.2 molal NaCl solution [6]. A difference exists in the position of the maximum of  $g_{\text{ClO}}(r)$  which is now centered at 3.18 Å as compared to 3.3 Å in the NaCl solution, which is a consequence of the newly calculated effective anion-water pair potential described above. A similar shift from 2.25 Å to 2.4 Å has been observed for the maximum position of  $g_{\text{ClH}}(r)$ . Any differences that could be

attributed to the influence of the different cations are not observed in  $g_{\text{ClO}}(r)$ . The coordination number of the anion can be evaluated as  $6.5 \pm 0.5$  from  $n_{\text{ClO}}(r)$  and  $n_{\text{ClH}}(r)$  at the position of the minimum — not well defined in  $g_{\text{ClO}}(r)$  — in the corresponding RDF's. This value is in good agreement with experimental results [2]. From the positions of the maxima in the two RDF's it is indicated that one hydrogen atom of every hydration shell water is preferentially pointing to the anion.

The oxygen-oxygen RDF for the 1.1 molal  $\text{MgCl}_2$  solution is shown in Figure 3. A comparison with the 2.2 molal NaCl solution shows a shift of the increasing part of the first peak in  $g_{\text{OO}}(r)$  to smaller values in the case of the  $\text{MgCl}_2$  solution. A more detailed investigation of certain water subsystems (e.g. hydration shell water) in respect to their contributions to the RDF of total water has led to the following results: The mean distances of a water molecule in the first hydration shell of magnesium and its neighbors in the first and second hydration shells are shortened to 2.76 Å and 2.70 Å, respectively. The origin for this shortening must be attributed to the electrostatic forces exerted from the ion on the water molecules. The number of nearest neighbors derived from the running integration number at the distance of 3.4 Å — the position of the minimum in  $g_{\text{OO}}(r)$  — for all water molecules is about  $n = 5.0 \pm 0.1$ . Taking into account only the neighbors of a water molecule which belongs to the first hydration shell of the cation, the mean number of neighbors up to a distance of 3.4 Å increases to 7.0 in spite of the excluded volume effect thus indicating the strong structure altering ability of the cation on the water molecules around. If these hydration shell waters of  $\text{Mg}^{++}$  are excluded, the remaining water molecules have on the average 4.6 nearest neighbors what is very close to



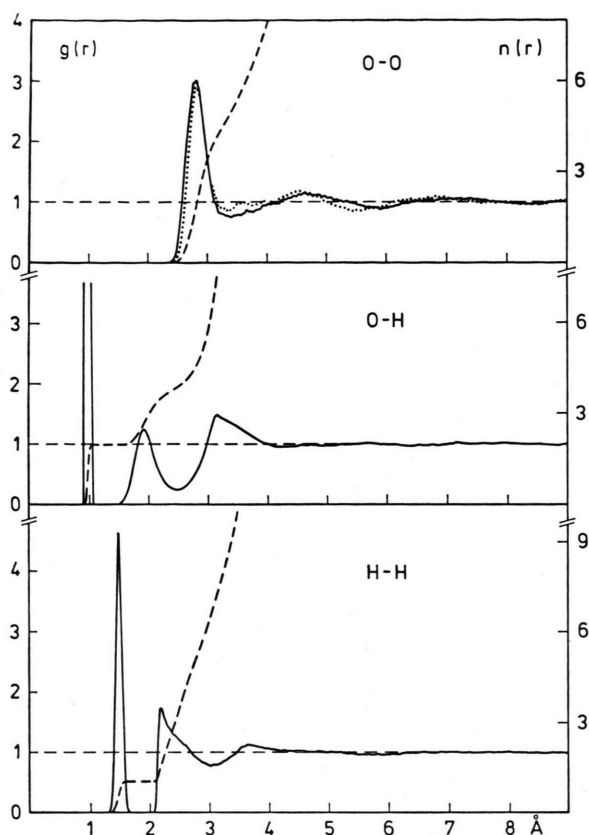


Fig. 3. Oxygen-oxygen, oxygen-hydrogen, and hydrogen-hydrogen radial distribution functions (full) and running integration numbers (dashed) for a 1.1 molal  $\text{MgCl}_2$  solution. The oxygen-oxygen radial distribution function of a 2.2 molal  $\text{NaCl}$  solution (dotted) is given for comparison.

the value found in the simulation of pure CF-water [5].

The first minimum in  $g_{\text{OO}}(r)$  is better established than in the case of the  $\text{NaCl}$  solution presumably caused by the arrangement of the hydration shell waters of the cation whose mean nearest neighbor distances are very similar to that of the other waters. In the range of  $r > 3.5 \text{ \AA}$  the RDF shows, similarly to the result of the  $\text{NaCl}$  solution, a far ranging structure characteristic for the CF-water model.

In the oxygen-hydrogen RDF — shown in Fig. 3 — the height of the first intermolecular peak has decreased compared to pure water and — less pronounced — compared to the  $\text{NaCl}$  solution. A reasonable explanation is an excluded volume effect: For the water molecules in the hydration shell of the cation the lone pair directions are occupied by the

ion instead of hydrogens. (The same effect was observed in a simulation of a 2.2 molal aqueous  $\text{LiCl}$  solution employing the rigid ST2-water-model [1].) The value of  $n_{\text{OH}}(r) = 4.0$  at the minimum after the first intermolecular peak is slightly greater than the corresponding value for the  $\text{NaCl}$  solution indicating a smaller excluded volume effect for the cation. This might be a consequence of the smaller number of cations.

The hydrogen-hydrogen RDF — shown in Fig. 3 — is very similar to that of the  $\text{NaCl}$  solution. Only the intramolecular peak is shifted to smaller values as a result of the influence of the cation on the geometry of the water molecules. This will be discussed below in more detail for the different water subsystems.

The ion-ion RDF's are not shown because of their large statistical uncertainty, although they indicate the existence of non-contact ion pairs between  $\text{Cl}^-$  and  $\text{Mg}^{++}$ .

#### B) Dipole Moments and Geometry of Water Molecules

As a general feature the effective dipole moments of molecules are increased in liquids compared to their gas phase values because of induction effects. This can be investigated with the CF model for water because of its non rigid geometry. In Fig. 4 the mean value of the magnitude of the water dipole moment is plotted against the ion-oxygen distance for  $\text{Mg}^{++}$  and  $\text{Cl}^-$ . Over the range of the first cation hydration shell there is a steep decrease which is

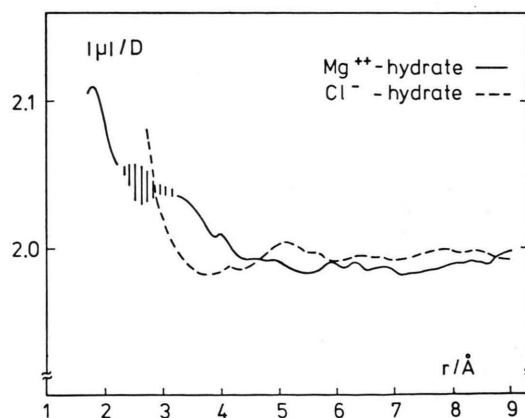


Fig. 4. Average value of the water dipole moment as a function of the ion-oxygen distance for  $\text{Mg}^{++}$  (full) and  $\text{Cl}^-$  (dashed) for a 1.1 molal  $\text{MgCl}_2$  solution.

continued in the second hydration shell up to about 4.5 Å with an interruption in the range between the two hydration shells where practically no water molecule is found. Behind the distance of 4.5 Å a nearly constant mean dipole moment is observed. In the case of the anion the dipole moment is decreasing similarly over the range of the hydration shell. But then a different behaviour is observed: the magnitude of the dipole moment reaches a minimum at about 3.7 Å and increases again to a maximum value at a distance of about 5 Å. A similar behaviour was observed in the NaCl solution. This might be explained in the following way: there is a good chance for those waters at 5 Å distance to the anion to belong simultaneously to the first or second hydration shell of the cation and thus getting an increased dipole moment compared to smaller distances at about 4 Å.

To elucidate the origin of the increased dipole moment of the water molecules around the ions their geometry was investigated. In Fig. 5 the distributions of the HOH-angles are shown for water molecules belonging to the first hydration shell of  $\text{Mg}^{++}$ ,  $\text{Cl}^-$ , and bulk water. Further contributions to the different dipole moments are stemming from the different OH-lengths depending upon the surroundings. The mean values for the HOH-angles and the OH-lengths are given in Table 3 together with the mean values for the intramolecular HH-distances and the dipole moments.

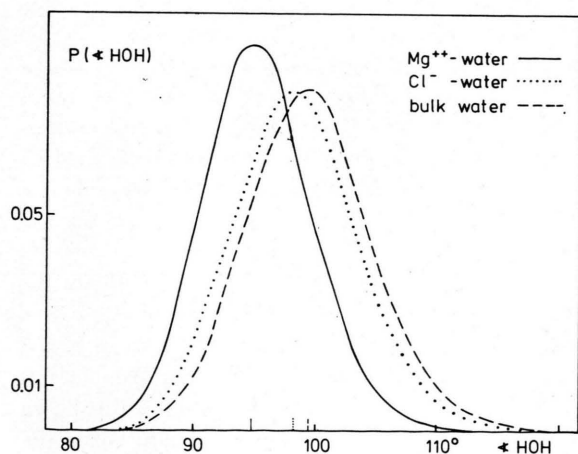


Fig. 5. Normalized distributions of the HOH-angle for hydration water of  $\text{Mg}^{++}$  (full),  $\text{Cl}^-$  (dotted), and bulk water in an 1.1 molal  $\text{MgCl}_2$  solution. The average values are marked on the abscissa.

Table 3. Average values of the dipole moments, HOH-angles, oxygen-hydrogen, and hydrogen-hydrogen distances for hydration water and bulk water molecules in the  $\text{MgCl}_2$  solution and in the NaCl solution. The values for the dipole moment and the HOH-angle in pure water are calculated from  $r_{\text{OH}}$  and  $r_{\text{HH}}$  taken from Figs. 3 and 4 in [5] and are therefore less accurate.

	$ \mu /\text{D}$	$\angle \text{HOH}/^\circ$	$r_{\text{OH}}/\text{\AA}$	$r_{\text{HH}}/\text{\AA}$
$\text{Mg}^{++}$	2.11	94.5	0.988	1.46
$\text{Na}^+$	2.00	99.3	0.975	1.49
$\text{Cl}^-(\text{Mg})$	2.01	98.5	0.980	1.48
$\text{Cl}^-(\text{Na})$	1.99	99.4	0.973	1.48
bulk(Mg)	2.00	99.2	0.975	1.49
bulk(Na)	1.98	99.9	0.973	1.49
pure [5]	(1.90)	(102)	0.96	1.5

As is demonstrated by the values in Table 3 the effect exerted by the ions on the water molecules around them consists of an increased oxygen-hydrogen distance combined with a smaller HOH-angle. This effect is strongest in the case of  $\text{Mg}^{++}$ , less in the case of  $\text{Na}^+$  and  $\text{Cl}^-$ . The differences between  $\text{Cl}^-$  and bulk in the case of the  $\text{MgCl}_2$  and the NaCl solution might be attributed to the influence of the twofold charge of the  $\text{Mg}^{++}$  which affects the water geometry also at distances outside the first hydration shell.

### C) Orientation of the Water Molecules

Additional information on the structure of the aqueous  $\text{MgCl}_2$  solution besides the RDF's is provided by the investigation of the orientation of the water molecules in the hydration shells in respect to the ions. Also the orientation of the water molecules in respect to a reference one will be discussed. The orientation of a water molecule in respect to an ion can be described by the cosine of the angle  $\theta$  between the dipole moment vector and the vector pointing from the oxygen to the ion.

In the well defined first hydration shell of the  $\text{Mg}^{++}$  an extremely sharp distribution is found with a maximum value of  $\cos \theta = -1.0$  and an average value of  $-0.941$  corresponding to an angle of  $160^\circ$  (Figure 6). We can compare this to the NaCl solution where the maximum of the distribution was also found at  $\cos \theta = -1.0$ , but this distribution was less sharp as indicated by an average value of  $-0.751$  corresponding to  $\theta = 140^\circ$ . This demonstrates very clearly the increased structuring ability of the twofold charged small ion on its hydration sphere.

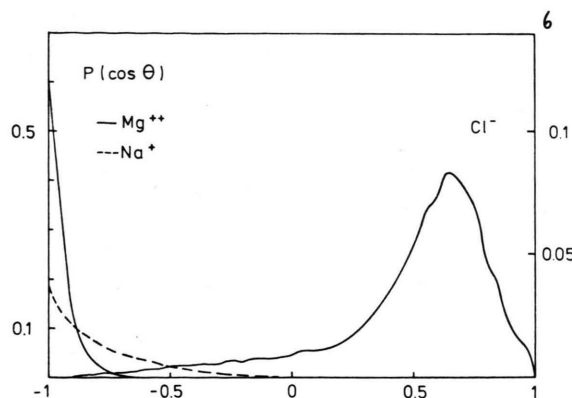


Fig. 6. Cosine distribution of the angle  $\theta$  between the vector pointing from the oxygen atom to the ion and the dipole moment vector of the water molecules in the first hydration shell of  $\text{Mg}^{++}$  and  $\text{Cl}^-$  (full) and, for comparison, of  $\text{Na}^+$  (dashed). The ordinate scale for  $\text{Cl}^-$  is on the rhs.

Even the second hydration shell of the  $\text{Mg}^{++}$  ion exhibits a preferential alignment of the water dipoles antiparallel to the oxygen-ion vector. The maximum of the  $\cos\theta$ -distribution is again found at  $\cos\theta = -1.0$  and the average value is  $-0.60$ . This means that a similar strength of the orientation of the water molecules is found for the first hydration shell of  $\text{Na}^+$  and the second one of  $\text{Mg}^{++}$ .

The radial dependance of  $\langle\cos\theta\rangle$  is shown in Figure 7. It is nearly constant over the range of the first hydration shell of the cation. In the first part of the second hydration shell — ranging from  $3.5 \text{ \AA}$  to about  $4.5 \text{ \AA}$  — there is only a slight decrease of the mean cosine, whereas at about  $4.5 \text{ \AA}$  (near to the second maximum of  $g_{\text{MgO}}(r)$ ) a rather steep loss of orientation is observed resembling the decay of  $\langle\cos\theta\rangle$  in the hydration shell of  $\text{Na}^+$ . It cannot be decided ultimately whether this is mainly caused by the surrounding water molecules or whether this reflects the influence of the anions disturbing the orientation of the water. There is a third region exhibiting preferential orientation from about  $6 \text{ \AA}$  up to about  $7.5 \text{ \AA}$  distance from the  $\text{Mg}^{++}$ . There is a connection between the loss of orientation in the range of the second hydration shell at about  $4.5 \text{ \AA}$  and the fact that the magnitude of the water dipole moments reaches at the same distance its final constant value.

The distribution of  $\cos\theta$  of the water molecules in the  $\text{Cl}^-$  hydration shell is also shown in Figure 6. The maximum value is  $\cos\theta = 0.63$  corresponding

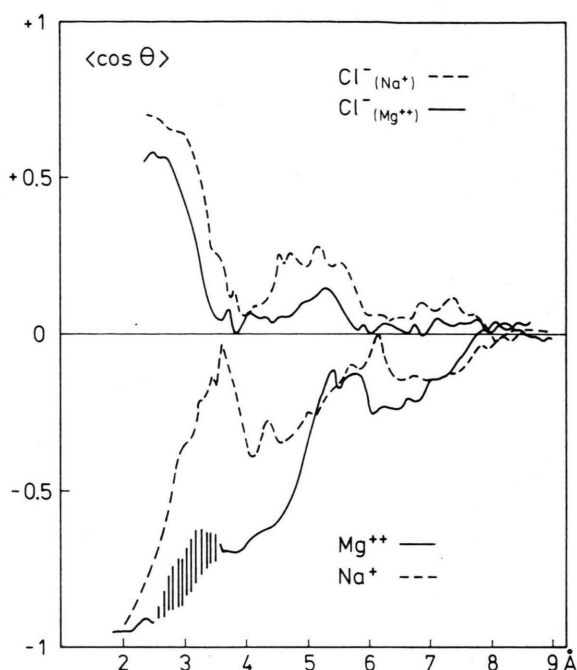


Fig. 7. Average values of  $\cos\theta$  as a function of the ion-oxygen distance for  $\text{Mg}^{++}$  and  $\text{Cl}^-$  (full) in the 1.1 molal  $\text{MgCl}_2$  solution. For comparison the values for  $\text{Na}^+$  and  $\text{Cl}^-$  (dashed) in the 2.2 molal  $\text{NaCl}$  solution are drawn.

to an angle  $\theta = 51^\circ$ . This result means that the water molecules are forming preferentially a nearly linear hydrogen bond with the anion.

A more detailed investigation on the orientation of the water molecules in the hydration shells of the ions will be published separately within the context of neutron diffraction experiments with isotopic substitution [14]. The variation of  $\langle\cos\theta\rangle$  with the distance from the ion is similar to what was found in the  $\text{NaCl}$  solution. The differences — less significant orientation of the water dipoles in the field of the anion in the  $\text{MgCl}_2$  solution — have to be attributed to the superimposed orientation in the field of the two-fold charged cation.

The average cosine of the angle  $\theta_{\text{ww}}$  between the dipole moment vectors of two water molecules as a function of their mutual distance is drawn in Fig. 8 for the 1.1 molal  $\text{MgCl}_2$  solution. For comparison the results for the 2.2 molal  $\text{NaCl}$  solution are shown as dashed line. In both curves there is a sharp decrease in the range of the first peak of  $g_{\text{OO}}(r)$  which is followed by a constant value up to  $5.5 \text{ \AA}$ . This far ranging structure was also observed in the corresponding RDF. For the  $\text{MgCl}_2$  solution smaller



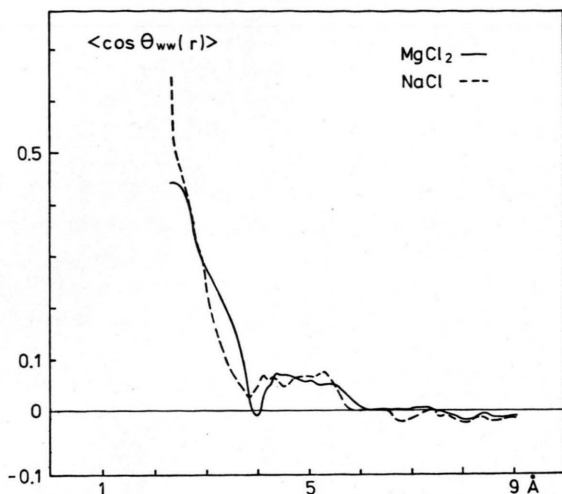


Fig. 8. Average value of the cosine between the dipole moments of two water molecules as a function of the oxygen-oxygen distance for the 1.1 molal MgCl<sub>2</sub> solution (full) and the 2.2 molal NaCl solution (dashed).

values are found at distances of 2.3 Å and 4.0 Å than for the NaCl solution. The differences at 2.3 Å shall not be discussed because they are based on a very small number of water molecules and thus have large statistical errors. As a detailed investigation assured, the differences at 4.0 Å are caused by the water molecules in the cation hydration shell which are on opposite sides of the cation and have an antiparallel orientation of their dipole moments. Their rather fixed orientations will cause a gap in the  $\langle \cos \theta_{ww} \rangle$  curve of the MgCl<sub>2</sub> solution. The negative cos-values at greater distances are artificial and will be discussed below.

Very closely related to the orientation of the water molecules is the dielectric constant [7]. There are, however, difficulties in the calculation of this quantity from computer simulations, which arise from the applied periodic boundary conditions. The method of the Ewald-Kornfeld summation for the electrostatic forces — which has been applied in this simulation — avoids the complete absence of electrostatic interactions for particles at distances greater than the cut off radius. But, nevertheless, the electrostatic interactions are also truncated, which causes the artificial mutual orientation between water molecules at distances greater than about 7 to 8 Å. These difficulties are under discussion and at the time no ultimate solution of this problem has yet been found.

In the Onsager-Kirkwood model the dielectric constant is connected to

$$f_k(r) = \langle \sum_j \cos \theta_{ij} \rangle, \quad (2)$$

where the summation extends over all water molecules "j" inside a sphere of radius  $r$ , surrounding a central water. The averaging extends over all water "i", which are in turn taken as central ones. For a sufficiently large sphere of non polarizable molecules imbedded in a medium of the same dielectric constant the relation is given by the Kirkwood formula

$$\frac{(\epsilon - 1)(2\epsilon + 1)}{\epsilon} = \frac{4\pi \rho \mu^2 f_k(r)}{kT}, \quad (3)$$

where  $\rho$  is the number density,  $k$  the Boltzmann constant,  $T$  the temperature, and  $\mu^2$  the average squared molecular dipole moment.

In Fig. 9  $f_k(r)$  is drawn as a function of the radius of the sphere for the 1.1 molal MgCl<sub>2</sub> solution and — for comparison — also for the 2.2 molal NaCl solution. The mean values of  $f_k(r)$  in the range of 4.5 Å to 9.1 Å (cut off distance) are  $\langle f \rangle = 3.5 \pm 0.4$  for the MgCl<sub>2</sub> solution and  $\langle f \rangle = 3.1 \pm 0.4$  for the NaCl solution. The values for the

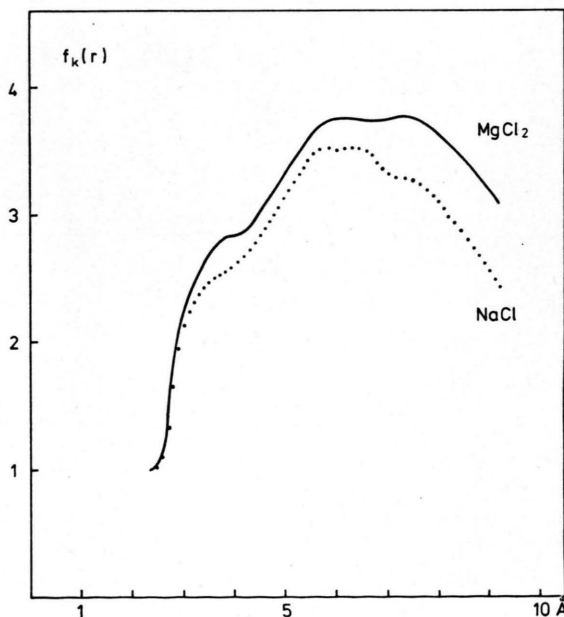


Fig. 9. Kirkwood-factor  $f_k(r)$  according to (2) as a function of the radius of the sphere surrounding a central water molecule for the 1.1 molal MgCl<sub>2</sub> and the 2.2 molal NaCl solution.

dielectric constant calculated according to (3) are  $\epsilon = 68 \pm 7$  for the  $\text{MgCl}_2$  solution and  $\epsilon = 60 \pm 7$  for the NaCl solution. The experimental values [15] are  $\epsilon = 65 \pm 2$  and  $\epsilon = 58 \pm 2$  for a 0.94 molal  $\text{MgCl}_2$  solution and a 2.0 molal NaCl solution, both at 298 K.

In respect to the possible incorrect application of the Kirkwood formula — there are different equations suggested in the literature for computer simulations, depending on the assumed dielectric properties of the space outside the sphere — and the somewhat arbitrary choice of the range from which  $\langle f \rangle$  has been calculated, the agreement might be fortuitous. The ratio of the calculated dielectric constants for the two solutions, however, is in the right order and should have more significance than the numerical values.

#### D) Average Potential Energies

The average potential energy  $\langle V(r) \rangle$  of a water molecule in the field of an ion as a function of the ion-oxygen distance for the  $\text{MgCl}_2$  solution is given in

Figure 10. Additionally  $\langle V(r) \rangle$  for  $\text{Na}^+$ -water in the NaCl solution is drawn. The positions of the first maxima in the corresponding RDF's (marked by arrows in Fig. 10) are found for both cations at slightly greater distances than the potential minima. This might result from the asymmetry of the average potential and — in the case of  $\text{Mg}^{++}$  — from the small space available for the hydration shell molecules. For the anion the minimum of the average potential energy and the position of the maximum of the RDF coincide. In this case the considerably greater radius of the anion provides enough space for the hydration water molecules to settle at the distance of the potential energy minimum.

The distribution for the potential energies for the water molecules in respect to a central ion are drawn in Figure 11. The highest probabilities (not drawn in Fig. 11) are found at  $-0.15$ ,  $-0.025$ , and  $-0.057 \cdot 10^{-12}$  erg with values of 0.11, 0.27, and 0.24 for  $\text{Mg}^{++}$ ,  $\text{Cl}^-$ , and  $\text{Na}^+$ , respectively. These peaks represent mainly the energies of water mole-

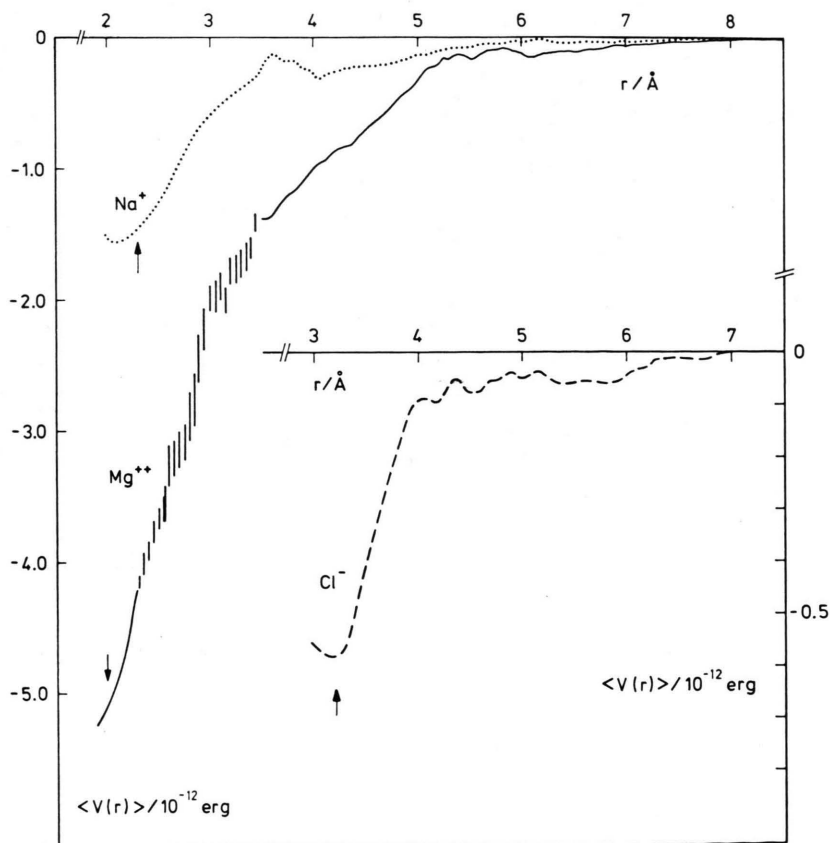


Fig. 10. Average potential energy of a water molecule in respect to a  $\text{Mg}^{++}$ -ion (full),  $\text{Cl}^-$ -ion (dashed), and  $\text{Na}^+$ -ion (dotted) as a function of the ion-oxygen distance. The positions of the maxima of the corresponding radial distribution functions are indicated by arrows.

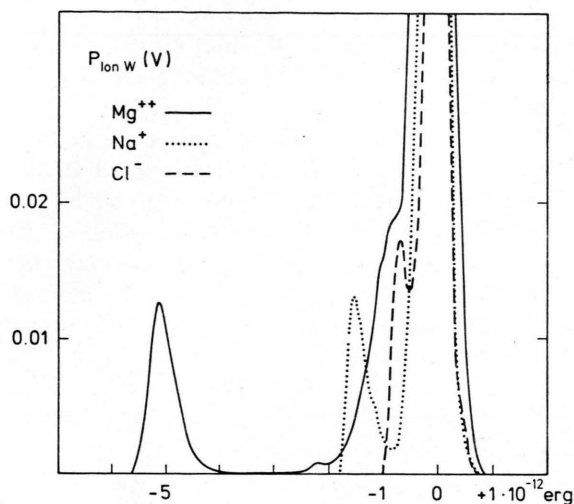


Fig. 11. Normalized distribution of the potential energies for  $\text{Mg}^{++}$ -water (full),  $\text{Cl}^-$ -water (dashed), and  $\text{Na}^+$ -water (dotted).

cules at greater distances from the ion. Therefore similar positions and widths of the peaks in the case of the single charged ions and a broader peak shifted to more negative values for the  $\text{Mg}^{++}$  are reasonable. The curve for  $\text{Mg}^{++}$ -water shows the energy distribution of the first hydration shell water as an isolated peak centered at  $-5.1 \cdot 10^{-12}$  erg. The following gap corresponds to the region between first and second hydration shell. The shoulder on the negative side of the main peak represents the energies of water molecules belonging to the second hydration shell. For  $\text{Na}^+$ -water the separation of the first hydration shell is less pronounced, as can be seen from the corresponding RDF. This causes, together with the less deep minimum in the potential energy curve, an only incomplete separation of the hydration shell water energies from the main peak. The energies of the second hydration shell waters are completely hidden in the main peak. Still less separation is found for the energy distribution of the  $\text{Cl}^-$ -hydration shell waters, only a small relative maximum is observable.

The integrated energies of hydration defined by

$$V_h(r) = 4\pi\epsilon_0 \int_0^r g_{\alpha\beta}(r') \langle V(r') \rangle r'^2 dr' \quad (4)$$

as a function of the ion-oxygen distance are shown in Fig. 12 for  $\text{Mg}^{++}$ -water,  $\text{Cl}^-$ -water, and for  $\text{Na}^+$ -water. The ranges with decreasing integrated hydration energy are obviously identical with the hydra-

tion shells as can be seen by comparison with the corresponding RDF's (Fig. 2) and the curves of the average cosine (Figure 7). Both cations show clearly a first and second hydration shell (Figure 12). The following regions, in which the energy decreases still by about 5% to 10% of the total amount, are of course influenced by the ions, but it would be overstressing to call them also hydration spheres. In the case of the anion the contribution behind the region of the first hydration sphere amounts to about 30% of the total energy. It is spread over a range from about 4 Å to 7 Å. In this range no structure in density is found (see Fig. 2) indicating a second hydration shell but the contribution of the  $\text{Cl}^-$ -water energy (see Fig. 10) — mainly stemming from electrostatic interaction — has not yet vanished.

In every case contributions to the hydration energy beyond an ion-oxygen distance of 8 Å can be neglected in accordance with the curves of the average potential energies. The following values (in kcal/mole) of the hydration energies for the differ-

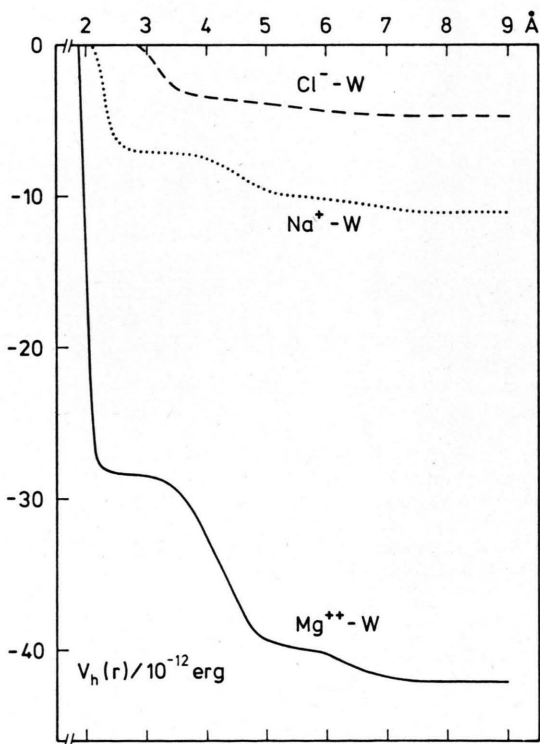


Fig. 12. Integrated energies of hydration for  $\text{Mg}^{++}$  (full),  $\text{Cl}^-$  (dashed), and  $\text{Na}^+$  (dotted) as a function of the ion-oxygen distance.



ent ions of the 1.1 molal  $\text{MgCl}_2$  solution and the 2.2 molal  $\text{NaCl}$  solution have been taken from the integrated hydration energy curves:

	$\text{Mg}^{++}$	$\text{Cl}^-$	$\text{Na}^+$
$-E_h$	610	68	160

### Acknowledgement

The authors are grateful to Dr. W. P. Kraemer and Dr. G. H. Dierksen for supplying their program MUNICH for the ab initio energy calculations for the  $\text{Mg}^{++}$ -water system. Financial support by Deutsche Forschungsgemeinschaft is gratefully acknowledged.

### Appendix A

There is a small number of ab initio studies on the system  $\text{Mg}^{++}\text{-H}_2\text{O}$  reported in the literature [10–12]. As the authors were interested mainly in dissociation energies all calculations have been carried out for structures with  $C_{2v}$ -symmetry. But for the derivation of a pair potential which describes as well as possible all  $\text{Mg}^{++}\text{-H}_2\text{O}$  arrangements appearing in a liquid, calculations for energetically unfavourable configurations are also necessary.

The calculations were carried out with the program system MUNICH [16] which uses Roothaan's SCF-MO-LCAO method [17]. The molecular orbitals are expanded into a set of gaussian orbitals which are contracted in order to reduce the number of linear parameters. The basis sets used in the calculations consist of (17s/8p)-functions contracted to (4p/2s), (13s/7p/1d)-functions contracted to (4s/2p/1d) [18], and (4s/1p)-functions contracted to (2p/1s) [19] centered at the  $\text{Mg}^{++}$ , oxygen and hydrogen, respectively. The geometry of the water molecule was kept fixed for all configurations with  $R(\text{O}-\text{H}) = 0.957 \text{ \AA}$  and  $\angle \text{HOH} = 104.52^\circ$ . We applied the closed shell approximation to get results compatible with the description of the analytical pair potential neglecting complexes like  $[\text{Mg}^+\text{H}_2\text{O}]^+$  [12].

The binding energies have been calculated with different ion-oxygen distances for planar water-ion arrangements at the angles  $\alpha = 0^\circ$ ,  $\alpha = 37.5^\circ$ ,  $\alpha = 90^\circ$ ,  $\alpha = 127.5^\circ$ , and  $\alpha = 180^\circ$  with  $\alpha$  defined as the angle between the vector pointing from the ion to the oxygen and the dipole moment vector of the water molecule. Additionally the energies for configurations with the  $\text{Mg}^{++}$  out of the water plane were calculated. The results for the planar configurations with  $\alpha = 0^\circ$  and  $\alpha = 37.5^\circ$  are shown in Figure 1.

- [1] Gy. I. Szász, K. Heinzinger, and W. O. Riede, *Z. Naturforsch.* **36a**, 1067 (1981).
- [2] R. Caminiti, G. Licheri, G. Piccaluga, and G. Pinna, *J. Appl. Cryst.* **12**, 34 (1979).
- [3] J. N. Albright, *J. Chem. Phys.* **56**, 3783 (1972).
- [4] A. K. Soper, G. W. Neilson, J. E. Enderby, and R. A. Howe, *J. Phys. C, Solid St. Phys.* **10**, 1793 (1977).
- [5] F. H. Stillinger and A. Rahman, *J. Chem. Phys.* **68**, 666 (1978).
- [6] P. Bopp, W. Dietz, and K. Heinzinger, *Z. Naturforsch.* **34a**, 1424 (1979).
- [7] J. G. Kirkwood, *J. Chem. Phys.* **7**, 911 (1939).
- [8] W. B. Streett, D. J. Tildesley, and G. Saville, *ACS Symposium Series* **86**, 144 (1978).
- [9] H. Kistenmacher, H. Popkie, and E. Clementi, *J. Chem. Phys.* **58**, 5627 (1973).
- [10] P. A. Kollmann and I. D. Kuntz, *J. Amer. Chem. Soc.* **94**, 9236 (1972).
- [11] A. Pullman, H. Berthod, and N. Gresh, *Int. J. Quantum Chem.* **10**, 59 (1976).
- [12] O. Blake, A. Les, and G. del Conde P., *J. Chem. Phys.* **73**, 5698 (1980).
- [13] G. Pálkás, T. Radnai, W. Dietz, Gy. I. Szász, and K. Heinzinger, *Z. Naturforsch.* **37a**, 1049 (1982).
- [14] Gy. I. Szász, W. Dietz, K. Heinzinger, G. Pálkás, and T. Radnai, to be published.
- [15] J. B. Hasted, D. M. Ritson, and C. H. Collie, *J. Chem. Phys.* **16**, 1 (1948).
- [16] G. H. F. Dierksen and W. P. Kraemer, Munich, Molecular Program System, Reference Manual, Special Technical Report, Max-Planck-Institut für Physik und Astrophysik, to be published.
- [17] C. C. Roothaan, *Rev. Mod. Physics* **23**, 69 (1951).
- [18] S. Huzinaga and Y. Sakai, *J. Chem. Phys.* **50**, 1371 (1969).
- [19] T. H. Dunning, *J. Chem. Phys.* **53**, 2323 (1970).